NeuroImage 58 (2011) 1028–1033

Contents lists available at ScienceDirect

NeuroImage

journal homepage: www.elsevier.com/locate/ynimg

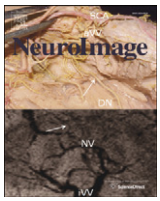

Orientation entropy analysis of diffusion tensor in healthy and myelopathic spinal cord

Jiao-Long Cui [1], Chun-Yi Wen [1], Yong Hu *,[1], Kin-Cheung Mak, Ka-Hung Henry Mak, Keith Dip-Kei Luk

Department of Orthopaedics and Traumatology, Li Ka Shing Faculty of Medicine, the University of Hong Kong, Hong Kong

ARTICLE INFO

Article history:
Received 16 January 2011
Revised 23 June 2011
Accepted 24 June 2011
Available online 18 July 2011

Keywords:
Cervical myelopathy
Spinal cord
Diffusion tensor imaging
Eigenvector
Orientation entropy

ABSTRACT

The majority of nerve fibers in the spinal cord run longitudinally, playing an important role in connecting the brain to the peripheral nerves. There is a growing interest in applying diffusion tensor imaging (DTI) to the evaluation of spinal cord microarchitecture. The current study sought to compare the organization of longitudinal nerve fibers between healthy and myelopathic spinal cords using entropy-based analysis of principal eigenvector mapping. A total of 22 subjects were recruited, including 14 healthy subjects, seven cervical myelopathy (CM) patients with single-level compression, and one patient suffering from multi-level compression. Diffusion tensor magnetic resonance (MR) images of the cervical spinal cord were obtained using a pulsed gradient, spin-echo echo-planar imaging (SE-EPI) sequence with a 3T MR system. Regions of interest (ROIs) were drawn manually to cover the spinal cord, and Shannon entropy was calculated in principal eigenvector maps. The results revealed no significant differences in orientation entropy values along the whole length of cervical spinal cord in healthy subjects (C2–3: 0.73 ± 0.05; C3–4: 0.71 ± 0.07; C4–5: 0.72 ± 0.048; C5–6: 0.71 ± 0.07; C6–7: 0.72 ± 0.07). In contrast, orientation entropy values in myelopathic cord were significantly higher at the compression site (0.91 ± 0.03), and the adjacent levels (above: 0.85 ± 0.03; below: 0.83 ± 0.05). This study provides a novel approach to analyze the orientation information in diffusion MR images of healthy and diseased spinal cord. These results indicate that orientation entropy can be applied to determine the contribution of each compression level to the overall disorganization of principal nerve tracts of myelopathic spinal cord in cases with multi-level compression.

Introduction

Magnetic resonance imaging (MRI) is currently the most widely used imaging technique for evaluating spinal cord parenchyma. However, conventional MRI, such as T1 and T2 weighted imaging, is limited to providing macroscopic information, including gross deformity and hemorrhage (Baron and Young, 2007a). Diffusion tensor imaging (DTI) was recently developed to enable the detection of tissue microarchitecture at the microscopic level based on a rank-two diffusion tensor model (Thurnher and Law, 2009). Commonly used parameters for delineation of spinal cord tissue microarchitecture include fractional anisotropy (FA), apparent diffusion coefficient (ADC) and mean diffusivity (MD). All of these parameters are derived from eigenvalues to evaluate the scalar properties of water molecule diffusion (Hagmann et al., 2006). Eigenvectors and eigenvalues derived from the diffusion tensor matrix respectively reflect the direction and strength of the movement of water molecules (Hagmann et al., 2006). The principal eigenvector indicates the dominant diffusion orientation of water molecules, which, in theory, is paralleled by the nerve bundles (Lin et al., 2001; Maier, 2007). The disturbance in the orientation of water molecule movement thus reflects the disorganization of nerve bundles. Although fiber tractography (FT) techniques have been developed for visualization of nerve bundles based on both eigenvalues and eigenvectors (Thurnher and Law, 2009), a mathematical approach for quantifying the severity of the disturbance in the orientation of water molecule movement is currently lacking.

Directional entropy has been proposed as a measure of the distribution of the dominant orientation of diffusion in the assessment of microstructural properties in the brain (Neuvonen and Salli, 2005). In our study, we want to introduce this entropy-based principal eigenvector analysis into the cervical spinal cord for evaluating microstructural changes after cervical myelopathy. It was postulated that such a method would be much more useful in the spinal cord than in the brain for detecting orientation changes, due to the orientational uniformity of spinal cord nerve tracts. In the present study, we measured orientation entropy as an index of disorder in orientation distribution, allowing us to examine a feature of cervical myelopathy (CM) after aligning single compression levels as the center. In addition, multiple level compression of the cervical spinal cord is common in CM. This poses a challenge for clinical diagnosis in determining the pathogenic level that should be targeted for surgical

* Corresponding author at: Dept. of Orthopeadics and Traumatology, The University of Hong Kong, 12 Sandy Bay Road, Pokfulam, Hong Kong. Fax: +852 29740335.
E-mail address: yhud@hku.hk (Y. Hu).
[1] The authors equally contribute to this work.

1053-8119/$ – see front matter © 2011 Elsevier Inc. All rights reserved.
doi:10.1016/j.neuroimage.2011.06.072

decompression to provide maximum benefit to patients with the fewest complications. We used feature extraction data in cases of confirmed CM to estimate the probabilities for pathogenic level along the multiple level compression cervical spinal cord in one case. These findings might help to guide treatment strategies for surgical decompression.

Materials and methods

Subjects

A total of 22 volunteers, including 11 males and 11 females ranging from 30 to 84 years of age, were recruited in this study with informed consent. All volunteers were screened to confirm their eligibility. The inclusion criteria of healthy subjects were intact sensory and motor function evaluated by the Japanese Orthopaedic Association (JOA) score system (Yonenobu et al., 2001), and negative Hoffman's sign under physical examination. Exclusion criteria included the presence neurological signs and symptoms, or a past history of neurological injury, diseases and operations. CM patients were recruited with confirmed diagnosis by senior spine surgeons with seven single level compression patients (four males, three females, aged 64 ± 20 years) and one multiple level compression patient (female, 58 years old). The healthy subjects were recruited as a control group ($n = 14$, aged 46 ± 16 years).

MR data acquisition

The procedures and protocols in this study were approved by the authors' Institutional Review Board (UW 04-104 T/246). All images were acquired with a 3.0T MR scanner (Achieva, Philips, Netherlands) with pulse sequence programming performed prior to scanning to optimize the image quality. During the acquisition process, the subject was placed supine using a SENSE neuro-vascular (SNV) head and neck coil enclosing the cervical region, and was instructed not to swallow to minimize the motion artifacts. The subject was then scanned for anatomical T1-weighted (T1W) images, T2-weighted (T2W) images and DTI.

Sagittal and axial T1W and T2W images were acquired for each subject using a fast spin-echo (FSE) sequence. For sagittal imaging, the imaging parameters were as follows: field of view (FOV) = 250 × 250 mm, slice thickness = 3 mm, slice gap = 0.3 mm, fold-over direction = feet/head (FH), number of excitation (NEX) = 2, resolution = $0.92 \times 1.16 \times 3.0$ mm^3 (T1W) and $0.78 \times 1.01 \times 3.0$ mm^3 (T2W), recon resolution = $0.49 \times 0.49 \times 3.0$ mm^3, and echo time (TE)/repetition time (TR) = 7.2/530 ms (T1W) and 120/3314 ms (T2W). A total of 11 sagittal images covering the whole cervical spinal cord were acquired. For axial imaging, the imaging parameters were as follows: FOV = 80×80 mm, slice thickness = 7 mm, slice gap = 2.2 mm, fold-over direction = anterior/posterior (AP), NEX = 3, resolution = $0.63 \times 0.68 \times 7.0$ mm^3 (T1W) and $0.63 \times 0.67 \times 7.0$ mm^3 (T2W), recon resolution = $0.56 \times 0.56 \times 7.0$ mm^3 (T1W) and $0.63 \times 0.63 \times 7.0$ mm^3 (T2W), and TE/TR = 8/1000 ms (T1W) and 120/4000 ms (T2W). Cardiac vectorcardiogram (VCG) triggering was applied to minimize the pulsation artifact from cerebrospinal fluid. Image acquisition began right after the rise of the wave of QRS complex. A total of 12 transverse images covering the cervical spinal cord from C1 to C7 were acquired, each of which was placed at the center of either a vertebra or an intervertebral disk. The pulse sequence used was single-shot spin-echo echo-planar imaging (SE-EPI). Diffusion encoding was performed in 15 non-collinear and non-coplanar diffusion directions with b-value = 600 s/mm^2. The imaging parameters were as follows: FOV = 80×80 mm, image matrix, 128×128, slice thickness = 7 mm, slice gap = 2.2 mm, fold-over direction = AP, NEX = 3, resolution = $1 \times 1.26 \times 7.0$ mm^3, recon resolution = $0.63 \times 0.63 \times 7.0$ mm^3, and TE/TR = 60 ms/5 heartbeats. The image slice planning was the same as in the anatomical axial T1W and T2W images, with 12 slices covering the cervical spinal cord from C1 to C7. The average duration of DTI was 24 min per subject, with an average heart rate of 60 beats per minute. Spatial saturation with spectral presaturation with inversion recovery (SPIR) was applied to suppress the fold-over effect. To alleviate EPI distortion problems caused by increased magnetic susceptibility at 3.0-T, the distortion correction method based on reversed gradient polarity and parallel imaging was employed (Andersson et al., 2003; Chuang et al., 2006; Morgan et al., 2004).

Data analysis for DTI and FT

Diffusion measurement was performed using DTI Studio software (Version 2.4.01 2003, Johns Hopkins Medical Institute, Johns Hopkins University, Baltimore, MD). Image volume realignment and 3D rigid body registration with different diffusion gradients were conducted using the Automated Image Registration (AIR) program (a source code embedded in DTI Studio software) to reduce the effect of motion artifact. The realigned and co-registered diffusion weighted data sets were double checked for image quality, then used for estimation of diffusion tensors, including three eigenvalues and the corresponding eigenvectors. The region of interest (ROI) was defined by B0 images to cover the spinal cord (Fig. 1) using Image J software (National Institute of Health, USA). For color coding of the eigenvector map in DTI Studio, each voxel is composed of three orthogonal direction components in an image reference frame: (r, g, b) – (ν_x, ν_y, ν_z), where r, g, and b represent red, green, and blue components of the voxel color, and (ν_x, ν_y, ν_z) is the normalized principal eigenvector, which points towards the coronal, axial and sagittal directions respectively (Jiang et al., 2006). The calculation of orientation entropy and least squares method (LSM) was performed using MATLAB (MathWorks, Natick, MA, USA).

Orientation entropy analysis

The eigenvector is a voxel-based measurement derived from the diffusion tensor so that the principal eigenvector only corresponds to the average fiber orientation within the voxel, and orthograde and retrograde directions of axonal tracts are not distinguished (Jiang et al., 2006). An angle resolution of 5° was used here, which was determined after comparison with other bin angles, including 3, 10, and 15°. Thus, the whole space was segmented as $K = (360°/5°) \times (90°/5°) = 1{,}296$ angle bands. The spatial direction pointed by the eigenvector in each voxel can be indicated by a pair of angles (θ, φ):

$$\text{Elevation angle } \theta = \sin^{-1}\left(\frac{\nu_z}{\sqrt{\nu_x^2 + \nu_y^2 + \nu_z^2}}\right)$$

$$\text{Azimuth angle } \varphi = \cos^{-1}\left(\frac{\nu_y}{\sqrt{\nu_x^2 + \nu_y^2}}\right).$$

The orientation entropy was defined in our study by

$$H = -\sum_{i=1}^{K} \frac{p(i)\ log_2[p(i)]}{log_2 N}$$

where $p(i)$ was the probability density that the eigenvector direction fell into the ith angle band, $\log_2 N$ was used to normalize the orientation entropy value to range from 0 (one orientation only) to 1 (all the orientations) where N was the number of the voxels covered. Orientation entropy does not identify the dominant orientation. Rather, it serves as an indicator of orientation spread or the scattering of eigenvector mapping (Neuvonen and Salli, 2005).

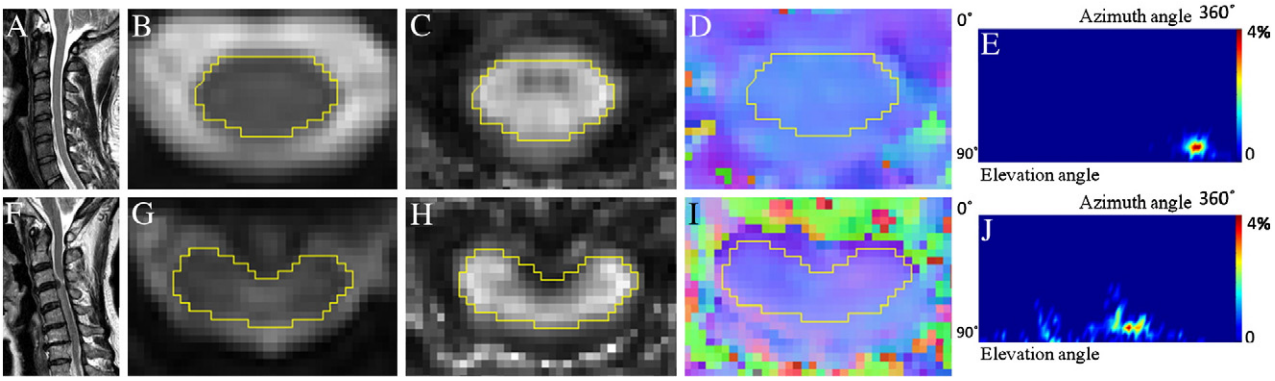

Fig. 1. The representative images showing sagittal T2W, B0, FA and principal eigenvector images in the healthy cord (A, B, C, D) and myelopathic cord (F, G, H, I). The ROI was defined by B0 image to cover the spinal cord. The 2D plot profile showed the directional distribution of eigenvectors included in the ROI (E, J). Orientation entropy value was 0.6464 and 0.9014 respectively in D and I. It was indicated that the orientational distribution in the myelopathic cord (J) was in a wider range than healthy cord (E), especially in-plane angle, corresponding to a higher orientation entropy value.

Least squares method for weight estimation

The method of least squares is a standard approach to the approximate solution for data fitting to minimize the sum of the squared residuals (Kailath, 1977). The least squares method (LSM) was used in the current study to estimate the weight w_i at each compression level. The increment of the orientation entropy value of unconfirmed myelopathy in multilevel compression can be written as

$$y(l) = \sum_{i \epsilon I} w_i x(l-i) + e$$

where I is the set of the compression levels, x is the increasing orientation entropy beyond the baseline in the extracted feature, l indicates the levels from C2 to C7 including five disk levels and six vertebral levels, and e is the residual between the predicted value and the actual value of the dependent variable. Therefore, to find the sum of squared residual minimum, the estimated weight based on LSM can be calculated as

$$\hat{w}_i = argmin\left\{ \sum_{l}^{L} \left[y(l) - \sum_{i \epsilon I} w_i x(l-i) \right]^2 \right\}.$$

Statistical analysis

Linear regression analysis was performed for normalization in order to eliminate the level-dependent discrepancy. Comparisons of orientation entropy value between healthy subjects and cervical myelopathy patients were performed using two-tailed *t*-test. The level of significance was set at $p<0.05$. All data analyses were performed using SPSS 15.0 analysis software (SPSS Inc, Chicago, IL, USA).

Results

Normalization of orientation entropy value along the length of cervical spinal cord

The orientation entropy values of 14 healthy subjects were used for statistical analysis along the whole cervical spinal cord. It was found that there was no significant difference between the upper cervical regions (C2–3: 0.7301 ± 0.0505, C3: 0.7276 ± 0.0495, and C3–4: 0.7080 ± 0.0660) and the lower regions (C5–6: 0.7128 ± 0.0746, C6: 0.7207 ± 0.0474, and C6–7: 0.7193 ± 0.0700) ($p>0.05$). Nevertheless, to eliminate the small discrepancies along the spinal cord, all orientation entropy values of both healthy subjects and cervical myelopathy patients were normalized to C2 level based on the result of linear regression analysis (Fig. 2). The horizontal fitting line after normalization (OE: 0.7191) was used as a normal baseline for feature extraction from cervical myelopathy.

Feature extraction of confirmed cervical myelopathy

The results showed that orientation entropy at the compression level as well as the two adjacent body levels and one disk level towards both cranial and caudal directions in the myelopathic cord were significantly higher than those of the healthy cord ($p<0.05$). Orientation entropy values in the myelopathic spinal cord were highest at the compression site(s) (OE(0): 0.9062 ± 0.0324) and decreased at the adjacent body and disk levels towards the cranial direction (OE(−1): 0.8543 ± 0.0270; OE(−2): 0.8240 ± 0.0461 and OE(−3): 0.7399 ± 0.0522) and caudal direction respectively (OE(1): 0.8290 ± 0.0510; OE(2): 0.8096 ± 0.0572 and OE(3): 0.7863 ± 0.0538).

To test the probability of pathogenic level estimation in the multiple level compression case, the mean increment of orientation entropy values (x(−3): 0.0208; x(−2): 0.1049; x(−1): 0.1352; x(0): 0.1871; x(1): 0.1099; x(2): 0.0905; x(3): 0.0672) were used as the feature of the confirmed myelopathy.

Estimation of the severity along the unconfirmed cervical myelopathy cord

T2W images revealed four compression sites in this case, which are C3–4, C4–5, C5–6 and C6–7 (Fig. 3). From the pattern of orientation entropy values, the weight at each compressive level for fitting this pattern was estimated using the least squares method (C3–4: 0.60; C4–5: 0.10, C5–6: 0.77 and C6–7: 0.43), and the squared residual was 0.0114. The estimated weight indicated the magnitude of pathological changes at each level in the multilevel compression cord in cervical myelopathy.

Discussion

This present study used quantitative measurement of the orientations of the fiber bundles in the spinal cord to examine microstructural disorganization in cases of cervical myelopathy. In addition, we applied orientation entropy to describe the orientation distribution of the nerve tracts in the cervical spinal cord in diffusion MR images. A feature of confirmed cervical myelopathy was extracted from single compression sites as well as adjacent levels by aligning the injured position as the center. An extracted myelopathy feature in a case of multi-level compression then estimated the probability of pathogenic level.

In the healthy spinal cord, orientation entropy values were consistently low, in accord with the neuroanatomy of spinal cord

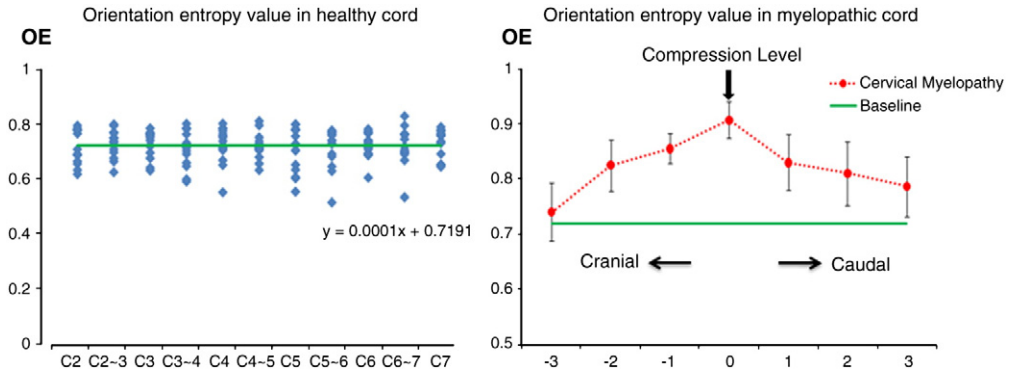

Fig. 2. Scatterplots of orientation entropy value in healthy cord and averaged value in myelopathic cord. In healthy cord, the dots indicated orientation entropy value along cervical spinal cord before normalization. The linear regression was performed to detect the trend of value changes along the cervical spinal cord and further eliminate the tiny level-dependant discrepancy. In myelopathic cord, the orientation value was calculated by aligning the compression level to extract the feature of cervical myelopathy. It was found that there was a peak at the compression level and the value decreased with the distance from the compression (dot line). The fitting result of orientation value in healthy cord after normalization was used as the baseline (solid line).

nerve tracts, in which the major of the fibers in the white matter run longitudinally (Tortora and Anagnostakos, 1993). The histogram in Fig. 1 showed that the spread of spatial direction in the healthy cord was concentrated, indicating that the orientation of the nerve tracts in the healthy spinal cord was highly ordered. In contrast, the orientation distribution in CM patients was distributed over a wide range. Correspondingly, orientation entropy values were higher in CM patients compared with healthy subjects at the compression and adjacent sites, implying microarchitectural changes, possibly due to demyelination, edema, or hemorrhage. In addition, we found that these changes also exhibited a specific pattern, by which the increment of the DE value peaked at the compression level and decreased with the distance along the cranial and caudal directions. This finding indicates that microstructural disorganization occurred most strongly at the compression level, and at adjacent levels in the cases of single compression.

To date, the pathophysiology of cervical myelopathy has been uncertain, widely considered to be a disorder characterized by compression of the cervical spinal cord or nerve roots within the spinal canal stenosis by varying degrees and involving a variable number of levels (Baron and Young, 2007b; McCormick et al., 2003). Cervical cord compression can occur as a result of disk herniation, the degeneration of the joints or ligaments, or osteophytic spurs (spondylosis). However, it has been reported that the clinical symptoms of CM patients are not associated with the compression ratio revealed by anatomical MRI images (Budzik et al., 2011; Matsumoto et al., 2000; Xiangshui et al., 2010). One study reported that pathological changes, such as changes in T1W or T2W image signal intensity, occurred at sites distant from the compression position (Baptiste and Fehlings, 2006; Baron and Young, 2007b). Moreover, the routine T1/T2 MR imaging techniques provide information only at the macroscopic level, such as edema, hemorrhage etc. There is mounting evidence that diffusion MR parameters, i.e. FA,

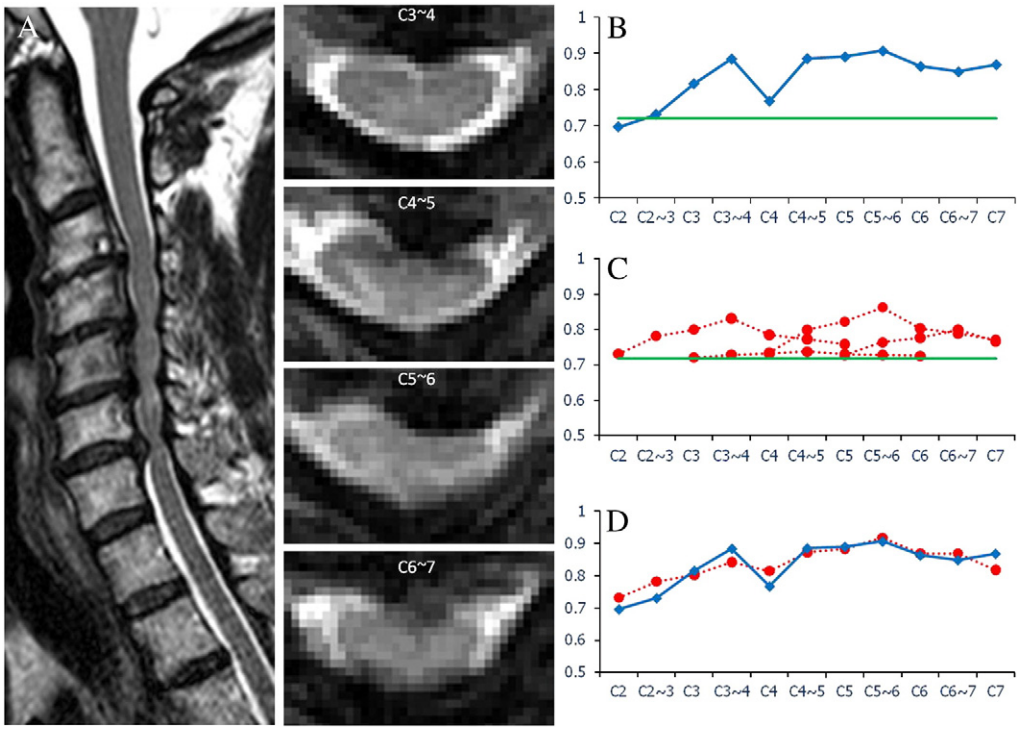

Fig. 3. Orientation entropy value compared with estimated value in the multilevel compression patient. The estimated value was a linear weighted sum of confirmed feature extracted from the single level compression cases (Fig. 2). A: The compression sites were shown by T2W image. B: Orientation entropy value along the whole cervical spinal cord in this patient (solid line). C: The weighting at each compression level was estimated under least squares method. D: The fitting effect was indicated by comparing the weighted sum (dash line) with the original orientation entropy value (solid line).

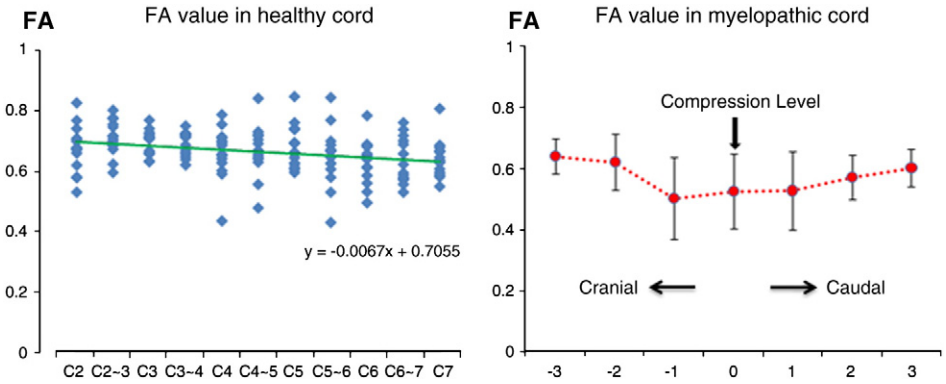

Fig. 4. Mean FA value within the ROI measured in the healthy cord and myelopathic cord. The trend line showed that the FA value decreased with the levels along the spinal cord from cranial to caudal direction in healthy cord. In myelopathic cord, the lowest FA value occurred at the adjacent level above compression level rather than the compression level.

MD, are more sensitive in showing microstructural abnormalities in cervical myelopathy than conventional T2W image (Demir et al., 2003). In human cervical myelopathy, these parameters have been widely investigated, for both research and clinical applications (Budzik et al., 2011; Demir et al., 2003; Facon et al., 2005; Jones et al., 2011; Kara et al., 2011; Song et al., 2011; Xiangshui et al., 2010). Our group has also used entropy for analysis of FA measurement in healthy and myelopathic spinal cords (Cui et al., 2011). However, these traditional diffusion parameters were derived from eigenvalues so that orientational information about the microstructural disorganization in the myelopathic cord could not be provided by these scalar measurements. Directional entropy was once used in the brain as a measure of disorder of the diffusion orientation diffusion distribution, to detect white matter integrity (Neuvonen and Salli, 2005). The concept of entropy was originally used in the field of information theory to describe the state of complexity in a system (Shannon and Weaver, 1949). Compared with the complex tissue architecture in the brain, the dominant orderly orientation of the nerve tracts in the spinal cord could be more suitable for entropy-based analysis to sensitively detect orientation changes.

To our limited knowledge, there are several advantages of orientation entropy over the commonly used parameter, i.e. FA, in spinal cord DTI studies. As shown in previous others' and our study, the FA value of healthy spinal cord decreased with the level along the spinal cord (Mamata et al., 2005). In contrast, orientation entropy describes the uniformity or variability of the water molecule movement direction, which should be consistent along the spinal cord. Theoretically, it makes it easier for orientation entropy to identify the exact location of disturbance of water molecules movement in spinal cord DTI in comparison with FA (Fig. 4).

In addition, we did not detect the statistically significant correlation between orientation entropy and FA values along cervical spinal cord. It indicated that the overall direction of diffusion tensor might be not necessarily associated with the shape of individual ellipsoid. In fact, traditional measurements (FA and MD values) respectively served as the ratio and the average of the diffusion strength towards three orthogonal directions. Even frequent use of these measures, however, would involve the limitation that they could not describe the overall diffusion properties of tissue due to the loss of information regarding of diffusion directions. Thus, orientation entropy could provide a relatively simple, yet meaningful measure for the orientation information of nerve tracts, complementary to traditional measurements.

Several limitations of the current study should be considered. First, the partial volume effect may have contaminated the voxels drawn within the ROI, causing a directional bias among the principal eigenvectors. Therefore, special care was taken to avoid the CSF partial volume effect and motion artifacts in ROI selection. Second, the method we used for fitting orientation entropy values in the multiple level compression case was simple linear superposition as the sum of the weighted feature patterns. However, it remains possible that interactive effects among the multiple compressions affected the results. In addition, the sample size of the single compression cases was relatively small. However, our results demonstrated that this sample size was sufficient to successfully extract features of myelopathy level in compression with adjacent levels. A longitudinal study is currently underway to detect changes of the clinical symptoms and the estimated pathological severity at each level over time. This might provide a valuable method for exploring the progress and pathophysiology of cervical myelopathy.

Acknowledgments

The study is supported by the General Research Fund of the University Grant Council of Hong Kong (771608M). The authors would like to thank Dr. Kin-Cheung Mak and Dr. Henry Mak for their assistance in patient recruitment and MRI scanning.

References

Andersson, J.L., Skare, S., Ashburner, J., 2003. How to correct susceptibility distortions in spin-echo echo-planar images: application to diffusion tensor imaging. Neuroimage 20, 870–888.
Baptiste, D.C., Fehlings, M.G., 2006. Pathophysiology of cervical myelopathy. Spine J. 6, 190S–197S.
Baron, E.M., Young, W.F., 2007a. Cervical spondylotic myelopathy: a brief review of its pathophysiology, clinical course, and diagnosis. Neurosurgery 60.
Baron, E.M., Young, W.F., 2007b. Cervical spondylotic myelopathy: a brief review of its pathophysiology, clinical course, and diagnosis. Neurosurgery 60, S35–S41.
Budzik, J.F., Balbi, V., Le Thuc, V., Duhamel, A., Assaker, R., Cotten, A., 2011. Diffusion tensor imaging and fibre tracking in cervical spondylotic myelopathy. Eur. Radiol. 21 (2), 426–433.
Chuang, T.C., Huang, T.Y., Lin, F.H., Wang, F.N., Juan, C.J., Chung, H.W., Chen, C.Y., Kwong, K.K., 2006. PROPELLER-EPI with parallel imaging using a circularly symmetric phased-array RF coil at 3.0 T: application to high-resolution diffusion tensor imaging. Magn. Reson. Med. 56, 1352–1358.
Cui, J.L., Wen, C.Y., Hu, Y., Li, T.H., Luk, K.D., 2011. Entropy-based analysis for diffusion anisotropy mapping of healthy and myelopathic spinal cord. Neuroimage 54, 2125–2131.
Demir, A., Ries, M., Moonen, C.T., Vital, J.M., Dehais, J., Arne, P., Caille, J.M., Dousset, V., 2003. Diffusion-weighted MR imaging with apparent diffusion coefficient and apparent diffusion tensor maps in cervical spondylotic myelopathy. Radiology 229, 37–43.
Facon, D., Ozanne, A., Fillard, P., Lepeintre, J.F., Tournoux-Facon, C., Ducreux, D., 2005. MR diffusion tensor imaging and fiber tracking in spinal cord compression. AJNR Am. J. Neuroradiol. 26, 1587–1594.
Hagmann, P., Jonasson, L., Maeder, P., Thiran, J.P., Wedeen, V.J., Meuli, R., 2006. Understanding diffusion MR imaging techniques: from scalar diffusion-weighted imaging to diffusion tensor imaging and beyond. Radiographics 26 (Suppl 1), S205–S223.
Jiang, H., van Zijl, P.C., Kim, J., Pearlson, G.D., Mori, S., 2006. DtiStudio: resource program for diffusion tensor computation and fiber bundle tracking. Comput. Methods Programs Biomed. 81, 106–116.
Jones, J., Lerner, A., Kim, P.E., Law, M., Hsieh, P.C., 2011. Diffusion tensor imaging in the assessment of ossification of the posterior longitudinal ligament: a report on preliminary results in 3 cases and review of the literature. Neurosurg. Focus 30, E14.

Kailath, T., 1977. Linear Least-Squares Estimation. Dowden, Hutchinson and Ross, Stroudsburg.
Kara, B., Celik, A., Karadereler, S., Ulusoy, L., Ganiyusufoglu, K., Onat, L., Mutlu, A., Ornek, I., Sirvanci, M., Hamzaoglu, A., 2011. The role of DTI in early detection of cervical spondylotic myelopathy: a preliminary study with 3-T MRI. Neuroradiology 53 (8), 609–616.
Lin, C.P., Tseng, W.Y., Cheng, H.C., Chen, J.H., 2001. Validation of diffusion tensor magnetic resonance axonal fiber imaging with registered manganese-enhanced optic tracts. Neuroimage 14, 1035–1047.
Maier, S.E., 2007. Examination of spinal cord tissue architecture with magnetic resonance diffusion tensor imaging. Neurotherapeutics 4, 453–459.
Mamata, H., Jolesz, F.A., Maier, S.E., 2005. Apparent diffusion coefficient and fractional anisotropy in spinal cord: age and cervical spondylosis-related changes. J. Magn. Reson. Imaging 22, 38–43.
Matsumoto, M., Toyama, Y., Ishikawa, M., Chiba, K., Suzuki, N., Fujimura, Y., 2000. Increased signal intensity of the spinal cord on magnetic resonance images in cervical compressive myelopathy. Does it predict the outcome of conservative treatment? Spine (Phila Pa 1976) 25, 677–682.
McCormick, W.E., Steinmetz, M.P., Benzel, E.C., 2003. Cervical spondylotic myelopathy: make the difficult diagnosis, then refer for surgery. Cleve. Clin. J. Med. 70, 899–904.
Morgan, P.S., Bowtell, R.W., McIntyre, D.J., Worthington, B.S., 2004. Correction of spatial distortion in EPI due to inhomogeneous static magnetic fields using the reversed gradient method. J. Magn. Reson. Imaging 19, 499–507.
Neuvonen, T., Salli, E., 2005. Characterizing diffusion tensor imaging data with directional entropy. Conf. Proc. IEEE Eng. Med. Biol. Soc. 6, 5798–5801.
Shannon, C.E., Weaver, W., 1949. The Mathematical Theory of Communication. University of Illinois Press, Urbana.
Song, T., Chen, W.J., Yang, B., Zhao, H.P., Huang, J.W., Cai, M.J., Dong, T.F., Li, T.S., 2011. Diffusion tensor imaging in the cervical spinal cord. Eur. Spine J. 20, 422–428.
Thurnher, M.M., Law, M., 2009. Diffusion-weighted imaging, diffusion-tensor imaging, and fiber tractography of the spinal cord. Magn. Reson. Imaging Clin. N. Am. 17, 225–244.
Tortora, G.J., Anagnostakos, N.P., 1993. Principles of Anatomy and Physiology, 7th ed. Harper & Row, New York, London.
Xiangshui, M., Xiangjun, C., Xiaoming, Z., Qingshi, Z., Yi, C., Chuanqiang, Q., Xiangxing, M., Chuanfu, L., Jinwen, H., 2010. 3 T magnetic resonance diffusion tensor imaging and fibre tracking in cervical myelopathy. Clin. Radiol. 65, 465–473.
Yonenobu, K., Abumi, K., Nagata, K., Taketomi, E., Ueyama, K., 2001. Interobserver and intraobserver reliability of the japanese orthopaedic association scoring system for evaluation of cervical compression myelopathy. Spine (Phila Pa 1976) 26, 1890–1894 discussion 1895.